Medicine®

OPEN

The distinguishable DNA whole genome methylation profile of 2 cases of pediatric precursor B acute lymphoblastic leukaemia (BCP ALL) with prodromal, preleukemic phase
A case report

Radosław Chaber, MD, PhD[a,*], Artur Gurgul, PhD[b], Grażyna Wróbel[c], Anna Tomoń, MD[a],
Sylwia Paszek, MSc[d], Natalia Potocka, MSc[d], Olga Haus[e], Monika Lejman, PhD[f], Kornelia Łach, MSc[a],
Tomasz Szmatoła, MSc[b], Igor Jasielczuk, MSc[b], Blanka Rybka, PhD[c], Renata Ryczan-Krawczyk, MSc[c],
Sylwia Stąpor, MSc[g], Krzysztof Ciebiera, MSc[h], Christopher J. Arthur, M.Chem., PhD[i], Izabela Zawlik[d,j]

Abstract

Rationale: A prolonged, prodromal phase before definitive paediatric precursor B acute lymphoblastic leukaemia (BCP ALL) diagnosis is rarely observed.

Patients concerns: In the first, the patient presented with an aplastic preleukemic phase, whilst the second presented with a rheumatic-like preliminary phase.

Diagnoses: The case reports of two patients with BCP ALL with a prodromal phase lasting a few weeks are presented.

Interventions and outcomes: DNA whole genome profile methylation analysis of bone marrow cells obtained at diagnosis revealed a pattern of methylation that was readily distinguishable from both healthy and standard course BCP ALL bone marrow samples.

Lessons: The biological implication of this observation remains unclear, with many differentially methylated loci involved in many processes like neurogenesis, cell projection organization and adhesion along with leucocyte activation and apoptosis. The prevalence and clinical significance of these methylation changes is unknown but this data indicates that the epigenetic basis of BCP ALL with a prolonged, prodromal phase requires a more detailed assessment.

Abbreviations: ALL = acute lymphoblastic leukemia, BM = bone marrow, CBC = complete blood count, DM = differentially methylated, ESR = erythrocyte sedimentation rate, PLT = platelet count, PP = prodromal phase, SC = standard course, WBC = white blood cells.

Keywords: BCP ALL, DNA methylation, pediatric, 2 cases

1. Introduction

Acute lymphoblastic leukaemia (ALL) onset is usually sudden with a short history. A prolonged, prodromal phase (PP) before definitive ALL diagnosis is rarely observed. ALL can be recognized by bone marrow (BM) biopsy/aspirate and/or peripheral blood smear examination. WHO criteria from 2008[1] state that to establish a diagnosis of ALL, more than 20% to 25% of the lymphoblasts in bone marrow (BM) must possess a diagnostic phenotype. In the unusual case, that a patient presents with fewer than 20% lymphoblasts in the BM and with no evidence of an extramedullary mass but demonstrates 1 of the known recurring cytogenetic abnormalities associated with ALL, the patient may be considered to have lymphoblastic leukaemia. The observation of fewer than 20% unequivocal lymphoblasts in

the BM should, however, also prompt a search for lymphoblastic lymphoma in an extramedullary location.[2,3]

Leukaemia initiation requires nucleotide sequence changes to occur, such as point mutations, amplifications or chromosome translocations. In concert with these genetic changes, disrupted epigenetic regulation (via DNA methylation, post-translational histone modifications, and interaction with non-coding RNA (miRNA or siRNA)) results in the abnormal expression of key genes responsible for cell proliferation and differentiation.[4]

The most common clinical symptoms of ALL in children are secondary to peripheral pancytopenia resulting from normal BM precursor displacement. Sometimes a clinical view is complemented by hepatosplenomegaly, lymphadenopathy, symptoms of the central nervous system, or testis involvement, persistent fever, weight-loss and bone pain (particularly limb pain). Usually, examination of BM aspirates reveals up to 70% to 100% undifferentiated cells which correspond to the lymphoblast precursors, making ALL diagnosis proven. Definitive diagnosis of ALL thus normally takes no more than 2-3 weeks from the time of the first symptoms presenting.

In our previous work, hierarchical clustering of whole-genome DNA methylation profiles obtained from BM cells aspirated at diagnosis of a group of 38 patients with pediatric B-cell precursor (BCP) ALL revealed 2 cases with noticeably different methylation profiles.[5] Detailed clinical analysis of these patients showed that both had preceding clinical symptoms of leukaemia many weeks before ALL diagnosis was established. This pre-leukemic phase with incomplete features was misleading and delayed treatment. Herein we present the case reports of these 2 children. We, therefore, sought to fully analyze the differences in CpG methylation sites between BCP ALL patients with the standard course (SC) (BCP ALL SC) and the 2 with incomplete feature PP (BCP ALL PP).

2. Materials and methods

2.1. Ethical statement

Ethics Committee approval was obtained from the Institutional Review Board of the Medical University of Lodz (number, RNN/226/11/KE). Informed consent has been obtained from parents/legal guardians of all the participating children. Furthermore informed written consent was obtained from the parents of the 2 patients presented in this case report for publication. The study protocol conforms to the ethical guidelines of the 1975 Declaration of Helsinki.

2.2. Whole genome DNA methylation profile analysis

In our previous study[5] material comprised 38 samples of BM obtained from patients with pediatric precursor-B acute lymphoblastic leukaemia, at the time of the final ALL diagnosis, and 4 control non-leukemic samples. The analysis of cytogenetic ALL subtypes revealed that among BCP ALL SC patients there were 2 cases of triploidy and 12 cases of hyperploidy which might serve as a control for the analyzed BCP ALL PP patients. The previous results also showed, that factors such as gender and age are not important confounders for the global methylation profile differentiation of pediatric leukaemia.[5] DNA was purified using QIAamp DNA Blood Mini Kit (QIAGEN), assessed for fragmentation by agarose gel electrophoresis and quantified using Qubit 2.0 fluorimeter (Thermo Fisher Scientific). CpG methylation analysis was performed using Illumina (San Diego, CA) MethylationEPIC BeadChip, allowing analysis of 850K sites per sample.

2.3. Data quality control and analysis

The raw intensity data were checked for quality using the BeadArray Controls Reporter software (Illumina) and analyzed using the ChAMP package pipeline.[7] First, probes with detection of P value <.01 and with fewer than 3 beads in at least 5% of samples per probe were excluded. Additionally, non-CpG probes, SNP-related probes, multi-hit probes and probes located on chromosome X and Y were also removed. Then, the beta values (the proportion of DNA methylation at a CpG site) for 753,390 sites were calculated and assessed for quality by evaluation of beta multidimensional scaling (MDS) and density plots across the study groups. A beta value of 0 represents a completely unmethylated CpG site and a beta value approaching 1 represents a fully methylated CpG site. Beta values were normalized using the BMIQ method.[8] Singular value decomposition (SVD)[9] was used to identify the most significant components of variation, including technical variation. Differential methylation analysis between groups was performed using the champ.(DMP) function which implements the limma package[10] to calculate the P value for differential methylation using a linear model. The obtained p-values were corrected for multiple testing using the Benjamini–Hochberg procedure.[11]

2.4. Functional genes annotation and analysis

The genes associated with specific differentially methylated (DM) sites were separated depending on CpG site location (promoter, gene body) and analyzed in terms of molecular functions, biological presses, cellular components, pathways and phenotypes using WebGestalt (WEB-based GEne SeT AnaLysis) toolkit,[12] exploiting information obtained from GO, KEGG, WikiPathways, Human Phenotype Ontology and PharmGKB databases. Over-representation tests were performed with respect to all known human genes (genome), identifying enriched categories with a corrected P value (false discovery rate [FDR]) lower than 0.05 and requiring at least 5 genes per enriched category.

2.5. Methylation assay performance and differential methylation analysis

The assay performance, as evaluated based on control probes and BeadArray Controls Reporter software, was satisfactory across all studied samples. After preliminary filtering, 753,390 probes beta values were normalized and the batch effect was evaluated using the SWD method.

The comparison of methylation level of 753,390 sites between the 2 cases with BCP ALL PP and BCP ALL SC samples allowed the identification of 11,854 DM CpGs (adj P < .05). Of the sites, 7239 were hypermethylated in cases with PP ALL with an average delta beta between groups of 0.224 (±0.109). The remaining 4615 sites were hypomethylated with a slightly lower absolute delta beta value of 0.170 (±0.071). Both hyper- and hypomethylated CpGs were distributed on all 22 autosomes and the number of CpG per chromosome ranged from 1203 on HSA1 to 145 on HSA21.

CpG context analysis showed that 2090 of DM sites were located in gene promoter regions (TSS200 and TSS1500), 1433 in genes 5′-UTR or first exon and 4770 within gene bodies. Most of the detected DM sites (7302; 61.6%) were located outside known CpG islands and remaining ones were positioned in islands (18.3%) or islands' shelves and shores (20.1%). The detailed analysis of distribution of hyper- and hypomethylated sites showed that hypermethylation in BCP ALL PP is more common within promoter regions (22.7% versus 9.7% of all DM CpGs) and

known CpG islands (27.9% versus 3.2%) whereas hypomethylation occurs more frequently in gene bodies (48.4% versus 35.0) and regions outside islands (open sea; 78.8 versus 50.6%). DM sites and their annotations are reported in Supplementary File 1, http://links.lww.com/MD/C552.

Hypothesizing that some of the sites DM between BCP ALL PP and BCP ALL SC may conform to the methylation profile found in healthy BM samples, an additional comparison was made with respect to control samples. This analysis allowed the identification 41,952 DM sites of which 1511 overlapped with sites differing with respect to BCP ALL SC (Supplementary File 2, http://links.lww.com/MD/C553). Most of these sites were hypermethylated with respect to the control (1094; 72.4%) with an average delta beta of 0.228. Most of the sites were also hypermethylated with respect to BCP ALL SC with samples (1008) with average delta beta of 0.234. The selected DM sites were scattered across all autosomes with the highest number located on the biggest chromosomes and in gene bodies (35.8%), intergenic regions (24.9%), and outside known CpG islands (50.6%).

Unsupervised hierarchical clustering of the samples based on probes differing between BCP ALL PP and both ALL BCP SC and the control samples shows a clear separation of the 2 BCP ALL PP methylation profiles from both remaining groups with higher similarity to BCP ALL SC cases (Fig. 1). Comparable results were obtained when principal component analysis (PCA) was applied to the same probes (Fig. 2). For further gene functions analysis, only CpGs differing in methylation level between BCP ALL SC and control were used. 0

3. Results

3.1. Patient 1

This patient is a 10-year-old male with a history of the growth hormone deficiency, at admission he was undergoing growth hormone supplementation therapy. The patient was initially referred to hematology due to abnormal complete blood count (CBC) values (initial values: hemoglobin (Hb) of 9.6 g/dL, leukocytes (WBC) of 0.69×10^9/L, neutrophils of 0.1×10^9/L, and a platelet count (PLT) of 121×10^9/L.). Examination of peripheral blood smears revealed no blast cells. For 2 weeks before admission, the patient presented with a refractory fever of up to 39°C despite receiving 10-days axetil cefuroxime. At admission, no clinical and laboratory signs of infection were presented (procalcitonin, CRP, erythrocyte sedimentation rate (ESR) were among normal range) except for a urine culture which revealed *Morganella morganii* species 10^6/µL. Physical examination, confirmed by imaging, revealed hepatomegaly (liver AP diameter up to 12 cm) without any other abnormalities. Piperacillin with tazobactam therapy was introduced with a good clinical response. There was a resolution of the fever and the urine culture became sterile. Despite this, CBC values remained abnormal.

With a presumptive diagnosis of leukaemia, after admission, BM aspirates were obtained for morphology, immunophenotype, and cytogenetic analysis. Morphologically the BM was hypocellular with a paucity of megakaryocytes, abnormal granulopoiesis, and containing up to 20% of blasts. The immunophenotyping revealed 2 populations. The first population of CD34+/CD19+ cells with co-expression of myeloid antigen CD66+ (80% cells from this population) representing 2,5% of the total nucleated cells. The second population of CD34-/CD19+ also with CD66+ (60% cells) represented up to 20% of the total nucleated cells. The BM biopsies were repeated 4 times every few days, but the BM smears picture was constantly hypocellular with lymphoblast percentage within the

range of 10% to 25%. A similar percentage of lymphoblasts were observed by trephine biopsy examination, which revealed fields with different lymphoblast content. More than 3 weeks after admission, a spontaneous increase of white blood cells (WBC 2.64×10^9/L) and platelets (PLT 363×10^9/L) in the peripheral blood was observed with domination of lymphocytes (69%) but still without undifferentiated cells in the peripheral blood smears. After a further 2 weeks (about 5 weeks after admission) BM aspiration revealed the typical picture of acute leukaemia with hypercellular BM. The total percentage of blasts was about 35% with phenotype CD34-, CD19+, CD10+, CD22+, CD52+, CD38+, HLA-DR+ with co-expression CD66+ (55% cells), and CD15+ (60% cells). Conventional cytogenetic analysis by G-banding revealed the presence of additional chromosomes 4, 6, 17, 18, 21, and excluded the crucial aberrations connected with BCR/ABL or MLL loci.

Finally, the diagnosis of BCP ALL was established about 7 to 8 weeks after the onset of first symptoms. The treatment according to ALL IC BFM 2009 protocol[6] for an intermediate risk group without central nervous system involvement was introduced. A good prednisone response was observed and he achieved haematological remission on the fifteenth day with minimal residual disease level 1.8×10^{-5}. Presently, the maintenance oral chemotherapy is being continued and the patient has stayed in complete remission for 22 months.

3.2. Patient 2

This patient is a 6-year-old male was presented to rheumatology unit with a 5 months history of bone pain in both legs. Irregular episodes of fever up to 39°C (with frequency once a week) with spontaneous remission began 1 month after the onset of the bone pains. A systemic connective tissue disease was suspected. Comprehensive diagnostics was implemented. Initial CBC included Hb of 11.7 g/dL, leukocytes (WBC) of 6.22×10^9/L, neutrophils of 1.95×10^9/L, and a PLT of 550×10^9/L. A peripheral blood smear revealed a slightly increased percentage of lymphocytes (66%) and monocytes (10%) with the presence of atypical lymphoid cells (2%). The levels of CRP protein and ferritin as ESR were increased reflecting the active inflammatory process. Unfortunately, BM aspiration during this prodromal symptom phase was not performed, so BM cellularity and blast cells percentage before establishing the formal diagnosis is unknown.

Three weeks later, after the exclusion of rheumatic disorders, the patient was referred to haematology with persistent clinical symptoms and stable values of CBC, CRP, ferritin, and ESR. Physical examination revealed no symptoms of infection, no lymphadenopathy or hepatosplenomegaly, the neurological status, skin and testes were normal. Manual examination of peripheral blood smear revealed the presence of undifferentiated cells (5%) therefore a BM aspiration was performed. Immunophenotypic analysis of the BM aspirates revealed 61% of precursor B lymphoblasts with the coexpression of the myeloid line (about 1/3 cells with CD33+). Genetic analysis of blasts revealed the presence of a complex karyotype with hypotriploidy (63~66 chromosomes), with rearrangements loci IGH and TCRAD. Due to traumatic lumbar puncture, the central nervous system status stayed unknown. Finally, the diagnosis of BCP ALL was established, and the patient was stratified to the intermediate risk group according to ALL IC BFM 2009 protocol.[6] A good prednisone response was observed and haematological remission on the fifteenth day with residual minimal disease $7,1 \times 10^{-3}$ was achieved. Presently the patient has been in complete remission for 38 months after diagnosis without BM transplantation.
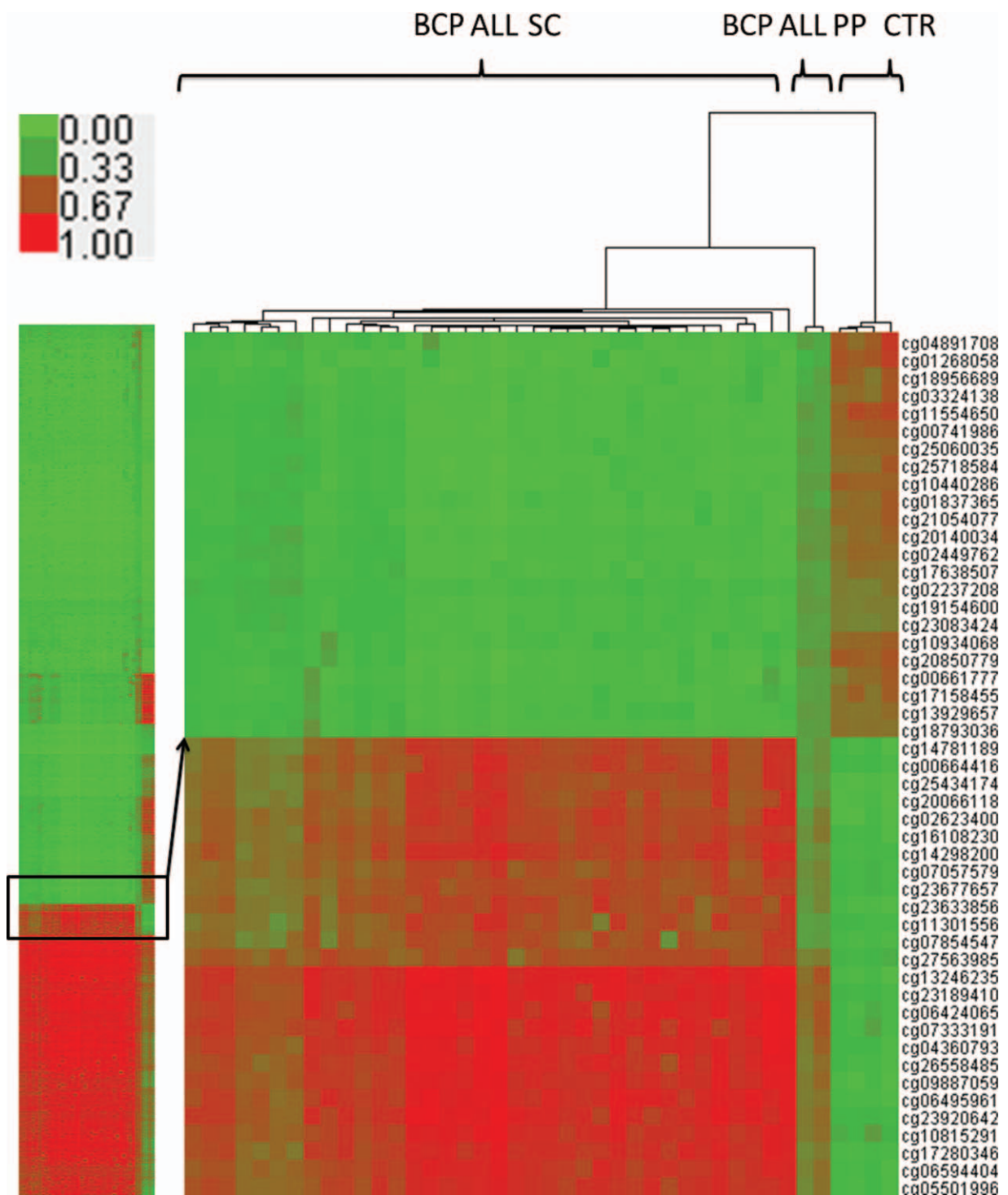
Figure 1. Hierarchical clustering of samples and methylation heatmap according to probes differing in methylation level between BCP ALL PP and both BCP ALL with the standard course (BCP ALL SC) and control samples.[5] BCP ALL PP = B-cell precursor acute lymphoblastic leukaemia with incomplete feature prodromal phase, SC = standard course.

4. Discussion

During our study of whole genome methylation changes within leukaemia methylation pattern across genome showed visible separation of the 2 samples profiles with clear differences with respect to control and BCP ALL SC patient groups. Detailed phenotypic analysis showed that these samples were obtained from cases of BCP ALL with few weeks duration PP before the confirmation of a formal diagnosis according to the WHO criteria. The first patient presented with an aplastic preleukemic phase, the second one with rheumatic-like preliminary phase. In both cases, treatment was delayed until the WHO criteria were fulfilled, so the "watch and wait" strategy was implemented. The
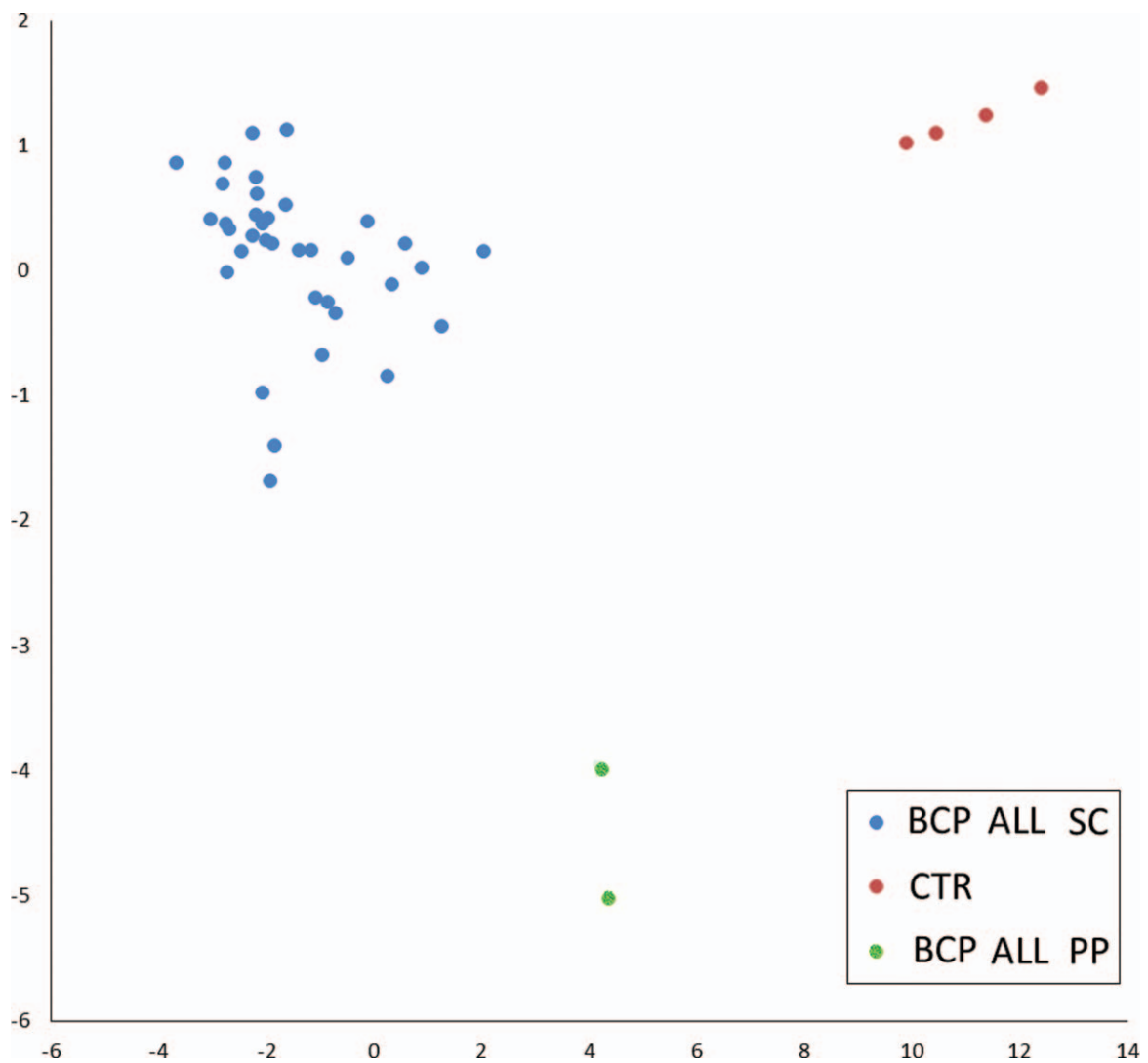
Figure 2. Principal component analysis based on probes differing in methylation level between B-cell precursor acute lymphoblastic leukaemia with incomplete feature prodromal phase (BCP ALL PP) and both BCP ALL with the standard course (BCP ALL SC) and control samples.[5] BCP ALL PP = B-cell precursor acute lymphoblastic leukaemia with incomplete feature prodromal phase, SC = standard course.

potential acceleration of leukaemia with its serious complications can be a reason for some concern for both patients and practitioners.

Aplastic PPs are rare but well recognized in childhood BCP ALL.[13–15] This neoplasm usually develops via a minimum of 2 discrete stages. First, the acquisition of chromosomal abnormalities (e.g., ETV6-RUNX1 fusion, high hyperdiploidy) predominantly (but not exclusively) during fetal hemopoiesis which drives the expansion of a clinically silent, or covert, but persistent preleukemic clone. Second, in a relatively small fraction of such cases, the accrual, postnatally of further, secondary genetic changes promote or precipitates disclosure of clinical leukaemia.[13,16,17] Occasionally, this form of ALL is initiated by infection, explaining the long-lasting remission due to induced, significant endogenous corticosteroids production.[6] The frequency of BCP ALL with preleukemic phase is low, and up to 2% of the ALL cases can be included in this group[14,18–20] while full symptomatic ALL appears after a sudden recuperation of the CBC, with 95% of cases progressing to ALL within 6 months of initial diagnosis.[21]

Musculoskeletal complaints that depend upon lymphoblast expansion in BM cavities may be the initial dominating symptoms of newly diagnosed leukaemia as well as rheumatic diseases, for example, juvenile idiopathic arthritis. It is extremely rare, however, to diagnose ALL in children with such complaints who were originally referred to a pediatric rheumatology unit (<1% of the all cases).[22–25] In these cases, the mean time between symptom onset and final diagnosis of leukaemia is about 3 months.[23]

The DM sites between BCP ALL PP and both BCP ALL SC and control samples were associated with 816 different genes. The genes were enriched in many GO biological processes which were summarized with the software package Revigo[26] to allow for the detection of their major categories (Table 1). Among the major classes of enriched biological processes are those associated, for example, with neurogenesis, cell projection organization and adhesion but also leukocyte activation and apoptosis.

The analyzed genes are also enriched in several KEGG pathways. Notably, these include T or B cell receptor signalling pathways, endometrial cancer or non-small cell lung cancer

Table 1

Major classes of biological processes enriched by genes with differentially methylated probes.

Term ID	Description	log10 P value
GO:0022008	Neurogenesis	−10.5784
GO:0030030	cell projection organization	−8.3665
GO:0006928	movement of cell or subcellular component	−7.5498
GO:0040011	Locomotion	−6.9318
GO:0043085	positive regulation of catalytic activity	−6.4841
GO:0022610	biological adhesion	−6.3605
GO:0007155	cell adhesion	−6.1739
GO:0046834	lipid phosphorylation	−5.7399
GO:0007267	cell-cell signaling	−5.7055
GO:0006357	regulation of transcription from RNA polymerase II promoter	−5.3449
GO:0001775	cell activation	−5.266
GO:0032970	regulation of actin filament-based process	−5.1361
GO:0048870	cell motility	−5.1163
GO:0051674	localization of cell	−5.1163
GO:0040007	Growth	−4.6968
GO:0009611	response to wounding	−4.5482
GO:0006915	apoptotic process	−4.4461
GO:0030029	actin filament-based process	−4.4202
GO:0008283	cell proliferation	−4.2161
GO:0018212	peptidyl-tyrosine modification	−3.9072
GO:0045321	leukocyte activation	−3.8081
GO:0016192	vesicle-mediated transport	−3.4564
GO:0014065	phosphatidylinositol 3-kinase signaling	−3.4381
GO:0044708	single-organism behavior	−3.2898
GO:0034332	adherens junction organization	−3.2697
GO:0035411	catenin import into nucleus	−3.2696
GO:0006897	Endocytosis	−3.1125

Major classes of biological processes enriched by genes with differentially methylated probes between B-cell precursor acute lymphoblastic leukemia with incomplete feature prodromal phase (BCP ALL PP) and both BCP ALL with the standard course (BCP ALL SC) and control samples. The numerous enriched biological processes found with WebGestalt were analyzed with Revigo system to summarize them by removing redundant GO terms.

(Table 2). The disease phenotypes enriched by the genes include acute myeloid leukaemia and Wiskott-Aldrich syndrome (Table 3).

Detailed analysis of the genes associated with the probes with the most significant differences in methylation level between BCP ALL PP and BCP ALL SC allowed the detection of 3 genes previously associated with the B cell phenotype, leukaemia or general tumour suppression and included: ENPP1, TCFL5, and LRRC3B genes.[27–29] The DM sites associated with ENPP1 gene were mainly located in the promoter region (TSS200) and were predominantly hypermethylated. For TCFL5 gene, the single DM sites were situated in TSS1500 (hypomethylated) and 1st exon (hypermethylated). In the case of the LRRC3B gene, the hypermethylated sites were distributed across the whole gene and were annotated to TSS200, 1st exon and 5'UTR.

To gain a better insight into the affected processes, the gene list was subdivided into 2 categories depending on the location of the probe within the gene body or promoter region (TSS200, TSS1500) as methylation in these areas may have opposite effect on the genes' expression. We identified 336 probes associated with the promoter

Table 2

KEGG pathways enriched by genes with differentially methylated probes.

	FDR	Involved genes
T cell receptor signaling pathway	0.000855	AKT3; MAP3K8; FYN; GRB2; LCK; NFATC1; NFATC2; PIK3CG; PIK3R2; PPP3R1; MAP2K1; VAV1; ZAP70; NCK2; CD28; GRAP2
Phospholipase D signaling pathway	0.006788	AKT3; RAPGEF4; DGKG; DGKH; DGKQ; DNM1; DNM2; FYN; GAB1; GRB2; CXCR2; PIK3CG; PIK3R2; MAP2K1; DGKZ; DGKD; CYTH1
Cholinergic synapse)	0.010435	AKT3; CHRM2; CHRNB4; FYN; GNGT2; KCNQ2; ACHE; PIK3CG; PIK3R2; PRKCG; MAP2K1; CREB3L2; CACNA1C; CAMK4
Endometrial cancer	0.012396	AKT3; ERBB2; GRB2; PIK3CG; PIK3R2; MAP2K1; TCF7; TCF7L1; CDH1
Non-small cell lung cancer	0.017792	AKT3; ERBB2; GRB2; PIK3CG; PIK3R2; PRKCG; MAP2K1; RXRA; TGFA
Phosphatidylinositol signaling system	0.020693	DGKG; DGKH; DGKQ; INPP1; INPP4A; INPP5A; PIK3CG; PIK3R2; PLCD1; PRKCG; DGKZ; DGKD
B cell receptor signaling pathway	0.020693	AKT3; GRB2; BLNK; NFATC1; NFATC2; PIK3CG; PIK3R2; PPP3R1; MAP2K1; VAV1
Adherens junction	0.020693	ERBB2; FER; FYN; SMAD3; NLK; TCF7; VCL; TCF7L1; ACTN1; CDH1
ErbB signaling pathway	0.020693	AKT3; ERBB2; GAB1; GRB2; PIK3CG; PIK3R2; PRKCG; MAP2K1; TGFA; NCK2; NRG2

Top 10 KEGG pathways enriched by genes with differentially methylated probes between B-cell precursor acute lymphoblastic leukemia with incomplete feature prodromal phase (BCP ALL PP) and both BCP ALL with the standard course (BCP ALL SC) and control.

Table 3

Disease phenotypes enriched by genes with differentially methylated probes.

	FDR	Involved genes
Adhesion	0.002432	*CDH4; CD96; EFNA5; SDK1; FER; ITGA11; ARHGAP26; FYN; CADM2; RGMB; GRB2; ICAM3; ITGA6; ITGAE; ITGAL; ITGB1; LAMB1; LIMS1; MGAT5; MYH9; NEO1; NRCAM; OLR1; PIK3CG; APBB1IP; STAB2; RADIL; PRKCE; PCDHGA4; PCDHA6; PCDHA2; RDX; RAPH1; SLC3A2; SVIL; TGFBI; TRIO; VCL; DDR1; NCK2; ACTN1; ARHGEF7; STARD13; CLDN10; CYTH1; NRXN2; CYTIP; PCDHGA8; CDH1*
Drug interaction with drug	0.002432	*PDIA5; ADD1; HSPB6; ADORA2A; ERBB2; F3; FYN; GAB1; SIN3A; GRB2; APP; ITGAL; ITGB1; KCNA4; KCNMA1; LCK; SMAD3; MAP1A; ACHE; PIK3CG; PIK3R2; PRKCE; PRKCZ; MAP2K1; RDX; RXRA; RYR2; S100A8; VAV1; ACTN1; ARHGEF7; ABCG2; BAG3; NCOR2*
Leukemia, Myeloid, Acute	0.009786	*CD96; MSI2; CSF3R; CUX1; DNMT3A; ETV6; ARHGAP26; SIN3A; GATA2; IRF8; MIR155; MPO; PBX1; MKL1; PRDM16; SECTM1; ZBTB16; ZNF496; ABCG2; BRE; NCOR2; CDA*
Ventricular Fibrillation	0.028874	*DPP6; KCNE1; KCNK3; RYR2; CACNA1C; CACNA2D1; EFCAB1; TANC1; KCNH7; NOS1AP*
Wiskott-Aldrich Syndrome	0.044225	*ABI2; WHAMM; DNM1; DNM2; FYN; GRB2; ITSN2; AMBRA1; ITSN1; NCK2; ARHGEF7; MTSS1L; MTSS1*
Developmental disorder NOS	0.049191	*DNM1; DYRK1A; AUTS2; FOXP1; HADHB; APP; KCNQ2; MAPT; MARK1; CHD7; MAP2K1; ARID1B; DCDC2C; NUAK1*

Disease phenotypes enriched by genes with differentially methylated probes between B-cell precursor acute lymphoblastic leukemia with incomplete feature prodromal phase (BCP ALL PP) and both BCP ALL with the standard course (BCP ALL SC) and control samples.

Table 4

Major classes of biological processes enriched by genes with differentially methylated probes located within gene bodies.

	Description	log10 *P* value
GO:0043087	regulation of GTPase activity	−7.5784
GO:0010647	positive regulation of cell communication	−6.0232
GO:0046834	lipid phosphorylation	−4.9747
GO:0030032	lamellipodium assembly	−4.7773
GO:0034330	cell junction organization	−4.7696
GO:0016192	vesicle-mediated transport	−4.382
GO:0032970	regulation of actin filament-based process	−4.2581
GO:0045216	cell-cell junction organization	−4.251
GO:0022603	regulation of anatomical structure morphogenesis	−4.2248
GO:0040011	Locomotion	−3.7327
GO:0007009	plasma membrane organization	−3.7188
GO:0006915	apoptotic process	−3.7024

Major classes of biological processes enriched by genes with differentially methylated probes located within gene bodies between B-cell precursor acute lymphoblastic leukemia with incomplete feature prodromal phase (BCP ALL PP) and both BCP ALL with the standard course (BCP ALL SC) and control samples. The numerous enriched biological processes found with WebGestalt were analyzed with Revigo to summarize them by removing redundant GO terms.

regions of 214 different genes. These genes did not enrich any of the GO biological processes, phenotypes or pathways. Analysis of the 445 genes associated with probes located in gene bodies was found to be enriched in a wide range of biological processes that could be reduced to major categories and are related to processes such as regulation of GTPase activity, positive regulation of cell communication or apoptotic processes (Table 4).

The genes with observed methylation differences within the gene bodies also enriched KEGG pathways associated with inter alia: non-small cell lung cancer, B cell receptor signalling pathway, endometrial cancer, renal cell carcinoma, and prostate cancer (Table 5). The diseases enriched by the genes included 3 phenotypes, namely: neoplastic cell transformation, adhesion aberration and Wiskott–Aldrich syndrome.

Kulis et al postulate that changes shared during neoplastic transformation and normal differentiation of lymphocytes B may represent epigenetic passengers whereas those exclusively taking place in tumour cells should contain epigenetic drivers with a potential functional impact in the disease.[30] The prevalence and clinical significance of the observed methylation changes, however, cannot be discerned from 2 patients alone. It is possible, however, to distinguish some differences in the DNA methylation profile between patients with BCP ALL PP and BCP ALL SC or individuals from the control group. No methylation changes were identifiable that could be obvious epigenetic drivers in these cases.

The frequency and implications of these methylation changes cannot be answered herein. Our data indicates, however, that the epigenetic basis of BCP ALL with an incomplete, prolonged, PP requires a more detailed assessment with a larger number of patients.

Author contributions

Conceptualization: Radosław Chaber, Christopher J. Arthur, Izabela Zawlik.

Formal analysis: Artur Gurgul, Tomasz Szmatoła, Igor Jasielczuk, Krzysztof Ciebiera, Christopher J. Arthur.

Investigation: Sylwia Paszek, Natalia Potocka, Monika Lejman, Kornelia Łach, Tomasz Szmatoła, Igor Jasielczuk, Krzysztof Ciebiera.

Methodology: Radosław Chaber, Artur Gurgul, Grażyna Wróbel, Anna Tomoń, Sylwia Paszek, Natalia Potocka, Olga Haus, Monika Lejman, Kornelia Łach, Tomasz Szmatoła, Igor Jasielczuk, Blanka Rybka, Renata Ryczan-Krawczyk, Sylwia Stąpor, Krzysztof Ciebiera, Christopher J. Arthur, Izabela Zawlik.

Table 5

KEGG pathways enriched by genes with differentially methylated probes within gene bodies.

	FDR	Involved genes
Non-small cell lung cancer	0.00074	AKT3; ERBB2; GRB2; PIK3CG; PIK3R2; PRKCG; MAP2K1; RXRA; TGFA
ErbB signaling pathway	0.00074	AKT3; ERBB2; GAB1; GRB2; PIK3CG; PIK3R2; PRKCG; MAP2K1; TGFA; NCK2; NRG2
B cell receptor signalling pathway	0.00074	AKT3; GRB2; BLNK; NFATC1; NFATC2; PIK3CG; PIK3R2; PPP3R1; MAP2K1; VAV1
EGFR tyrosine kinase inhibitor resistance	0.001425	AKT3; ERBB2; GAB1; GRB2; PIK3CG; PIK3R2; PRKCG; MAP2K1; TGFA; NRG2
Endometrial cancer	0.001579	AKT3; ERBB2; GRB2; PIK3CG; PIK3R2; MAP2K1; TCF7; CDH1
T cell receptor signaling pathway	0.001748	AKT3; GRB2; NFATC1; NFATC2; PIK3CG; PIK3R2; PPP3R1; MAP2K1; VAV1; NCK2; CD28
Phospholipase D signaling pathway	0.006316	AKT3; RAPGEF4; DGKH; DNM1; DNM2; GAB1; GRB2; PIK3CG; PIK3R2; MAP2K1; DGKZ; DGKD
Renal cell carcinoma	0.006325	AKT3; EPAS1; GAB1; GRB2; PIK3CG; PIK3R2; MAP2K1; TGFA
Prostate cancer	0.008014	AKT3; ERBB2; GRB2; PIK3CG; PIK3R2; MAP2K1; CREB3L2; TCF7; TGFA
Adherens junction	0.009944	ERBB2; FER; SMAD3; NLK; TCF7; VCL; ACTN1; CDH1
Acute myeloid leukemia	0.009944	AKT3; GRB2; PIK3CG; PIK3R2; MAP2K1; TCF7; ZBTB16
Bacterial invasion of epithelial cells	0.012155	DNM1; DNM2; GAB1; PIK3CG; PIK3R2; VCL; ARHGAP10; CDH1
VEGF signalling pathway	0.012395	AKT3; NFATC2; PIK3CG; PIK3R2; PPP3R1; PRKCG; MAP2K1
Regulation of actin cytoskeleton	0.012395	IQGAP2; FGF6; ITGA11; ITGA6; ITGAE; ITGAL; PIK3CG; PIK3R2; MAP2K1; RDX; VAV1; VCL; ACTN1; ARHGEF7
Choline metabolism in cancer	0.012395	AKT3; DGKH; GRB2; PIK3CG; PIK3R2; PRKCG; MAP2K1; DGKZ; DGKD
Pancreatic cancer	0.015854	AKT3; ERBB2; SMAD3; PIK3CG; PIK3R2; MAP2K1; TGFA
Glioma	0.015854	AKT3; GRB2; PIK3CG; PIK3R2; PRKCG; MAP2K1; TGFA
Natural killer cell mediated cytotoxicity	0.022128	GRB2; ITGAL; NFATC1; NFATC2; PIK3CG; PIK3R2; PPP3R1; PRKCG; MAP2K1; VAV1
Fc gamma R-mediated phagocytosis	0.024693	AKT3; DNM2; PIK3CG; PIK3R2; PRKCE; PRKCG; MAP2K1; VAV1
cGMP-PKG signaling pathway	0.03022	AKT3; KCNMA1; NFATC1; NFATC2; PIK3CG; PIK3R2; PPP3R1; PRKCE; MAP2K1; CREB3L2; CACNA1C
Sphingolipid signaling pathway	0.03022	AKT3; CERS6; PIK3CG; PIK3R2; PPP2R5C; PRKCE; PRKCG; MAP2K1; NSMAF
Phosphatidylinositol signaling system	0.031137	DGKH; INPP5A; PIK3CG; PIK3R2; PLCD1; PRKCG; DGKZ; DGKD
Hepatitis B	0.031137	AKT3; GRB2; SMAD3; NFATC1; NFATC2; PIK3CG; PIK3R2; PRKCG; MAP2K1; CREB3L2
AGE-RAGE signaling pathway in diabetic complications	0.033064	AKT3; F3; SMAD3; NFATC1; PIK3CG; PIK3R2; PLCD1; PRKCE
Focal adhesion	0.037454	AKT3; ERBB2; ITGA11; GRB2; ITGA6; PIK3CG; PIK3R2; PRKCG; MAP2K1; VAV1; VCL; ACTN1
Colorectal cancer	0.038715	AKT3; SMAD3; PIK3CG; PIK3R2; MAP2K1; TCF7
Osteoclast differentiation	0.04322	AKT3; GRB2; BLNK; NFATC1; NFATC2; PIK3CG; PIK3R2; PPP3R1; MAP2K1
Dorso-ventral axis formation	0.04322	ETV6; GRB2; ETV7; MAP2K1
Thyroid cancer	0.047349	MAP2K1; RXRA; TCF7; CDH1
Cholinergic synapse	0.047349	AKT3; CHRNB4; PIK3CG; PIK3R2; PRKCG; MAP2K1; CREB3L2; CACNA1C

KEGG pathways enriched by genes with differentially methylated probes within gene bodies between B-cell precursor acute lymphoblastic leukemia with incomplete feature prodromal phase (BCP ALL PP) and both BCP ALL with the standard course (BCP ALL SC) and control samples.

References

[1] Swerdlow SH, Campo E, Harris NL, et al. WHO Classification of Tumours of Haematopoietic and Lymphoid Tissues, Fourth Edition. IARC WHO Classification of Tumours, No 2. Lyon, France: IARC Press; 2008.

[2] Vardiman JW, Thiele J, Arber DA, et al. The 2008 revision of the World Health Organization (WHO) classification of myeloid neoplasms and acute leukemia: rationale and important changes. Blood 2009;114:937–51.

[3] Chiaretti S, Zini G, Bassan R. Diagnosis and subclassification of acute lymphoblastic leukemia. Mediterr J Hematol Infect Dis 2014;6: e2014073.

[4] Dawson MA, Kouzarides T. Cancer epigenetics: from mechanism to therapy. Cell 2012;150:12–27.

[5] Chaber R, Gurgul A, Wróbel G, et al. Whole-genome DNA methylation characteristics in pediatric precursor B cell acute lymphoblastic leukemia (BCP ALL). PLoS One 2017;12:e0187422.

[6] Campbell M, Castillo L, Riccheri C, et al. A Randomized Trial of the IBFM-SG for the Management of Childhood non-B Acute Lymphoblastic Leukemia Final Version of Therapy Protocol from August-14-2009. ALL IC-BFM. Available at: http://www.bialaczka.org/wp-content/uploads/2016/10/ALLIC_BFM_2009.pdf Accessed 2018/09/29.

[7] Morris TJ, Butcher LM, Teschendorff AE, et al. ChAMP: 450k chip analysis methylation pipeline. Bioinformatics 2014;30:428–30.

[8] Teschendorff AE, Marabita F, Lechner M, et al. A beta-mixture quantile normalization method for correcting probe design bias in illumina infinium 450 k dna methylation data. Bioinformatics 2013;29:189–96.

[9] Teschendorff AE, Menon U, Gentry-Maharaj A, et al. An epigenetic signature in peripheral blood predicts active ovarian cancer. PLoS One 2009;4:e8274.

[10] Smyth GK. Gentleman R, Carey V, Dudoit S, et al. Limma: Linear models for microarray data. Bioinformatics and Computational Biology Solutions Using R and Bioconductor New York, NY, Inc, Springer:2005;397–420.

[11] Benjamini Y, Hochberg Y. Controlling the false discovery rate: a practical and powerful approach to multiple testing. J R Stat Soc Ser B Methodol 1995;57:289–300.

[12] Zhang B, Kirov SA, Snoddy JR. WebGestalt: an integrated system for exploring gene sets in various biological contexts. Nucleic Acids Res 2005;33:W741–748.

[13] Horsley SW, Colman S, McKinley M, et al. Genetic lesions in a preleukemic aplasia phase in a child with acute lymphoblastic leukemia. Genes Chromosomes Cancer 2008;47:333–40.

[14] Breatnach F, Chessells JM, Greaves MF. The aplastic presentation of childhood leukaemia: a feature of common-ALL. Br J Haematol 1981; 49:387–93.

[15] Hasle H, Heim S, Schroeder H, et al. Transient pancytopenia preceding acute lymphoblastic leukemia (pre-ALL). Leukemia 1995;9:605–8.

[16] Greaves MF, Wiemels J. Origins of chromosome translocations in childhood leukaemia. Nat Rev Cancer 2003;3:639–49.

[17] Greaves MF, Maia AT, Wiemels JL, et al. Leukemia in twins: lessons in natural history. Blood 2003;102:2321–33.

[18] Sills RH, Stockman JA3rd. Preleukemic states in children with acute lymphoblastic leukemia. Cancer 1981;48:110–2.

[19] Schaison G. Acute curable preleukemic bone marrow aplasia in children. Biomed Pharmacother 1982;36:74–6.

[20] Armata J, Grzeskowiak-Melanowska J, Balwierz W, et al. Prognosis in acute lymphoblastic leukemia (ALL) in children preceded by an aplastic phase. Leuk Lymphoma 1994;13:517–8.

[21] Matloub YH, Brunning RD, Arthur DC, et al. Severe aplastic anemia preceding acute lymphoblastic leukemia. Cancer 1993;71:264–8.

[22] Zombori L, Kovacs G, Csoka M, et al. Rheumatic symptoms in childhood leukaemia and lymphoma-a ten-year retrospective study. Pediatr Rheumatol Online J 2013;11:20.

[23] Trapani S, Grisolia F, Simonini G, et al. Incidence of occult cancer in children presenting with musculoskeletal symptoms: a 10-year survey in a pediatric rheumatology unit. Semin Arthritis Rheum 2000;29:348–59.

[24] Gonçalves M, Terreri MT, Barbosa CM, et al. Diagnosis of malignancies in children with musculoskeletal complaints. Sao Paulo Med J 2005;123:21–3.

[25] Dorronsoro Martín I, Merino Muñoz R, Sastre-Urguellés A, et al. Malignant disease presenting as rheumatic manifestations. An Pediatr (Barc) 2004;61:393–7.

[26] Supek F, Bošnjak M, Škunca N, et al. REVIGO summarizes and visualizes long lists of gene ontology terms. PLoS One 2011;6:e21800.

[27] Yoon J, Wang H, Kim YC, et al. Plasma cell alloantigen ENPP1 is expressed by a subset of human B cells with potential regulatory functions. Immunol Cell Biol 2016;94:719–28.

[28] Silveira VS, Scrideli CA, Moreno DA, et al. Gene expression pattern contributing to prognostic factors in childhood acute lymphoblastic leukemia. Leuk Lymphoma 2013;54:310–4.

[29] Haraldson K, Kashuba VI, Dmitriev AA, et al. LRRC3B gene is frequently epigenetically inactivated in several epithelial malignancies and inhibits cell growth and replication. Biochimie 2012;94:1151–7.

[30] Kulis M, Merkel A, Heath S, et al. Whole-genome fingerprint of the DNA methylome during human B-cell differentiation. Nature Genet 2015;47:746–56.